Bull Volcanol (1993) 55:547–565

Bulletin of Volcanology

Evolution of a vent-hosted hydrothermal system beneath Ruapehu Crater Lake, New Zealand

B. W. Christenson, C. P. Wood

Wairakei Research Centre, Inst. Geological and Nuclear Sciences, Private Bag 2000, Taupo, New Zealand

Received: April 22, 1992/Accepted: August 5, 1993

Abstract. A two-year chemical monitoring program of Ruapehu Crater Lake shows that it has evolved considerably since the volcano's more active eruptive periods in the early 1970s. The present pH (20° C) of 0.6 is about one half unit more acid than the baseline values in the 1970s, whereas S/Cl ratios have increased markedly owing in part to declining HCl inputs into the lake, but also to absolute increases in SO_4 levels which now stand at the highest values ever recorded. Increases in K/Mg and Na/Mg ratios over the 20-year period are attributed to hydrothermal reaction processes in the vent which are presently causing dissolution of previously formed alteration phases such as natroalunite. These observations, combined with results of a recent heat budget analysis of the lake, have led to the development of a hydrothermal convection model for the upper portion of the vent. Possible vent/lake chemical reaction processes between end member reactants have been modelled with the computer code CHILLER. The results are consistent with the view that variations in lake chemistry, which are initiated by the introduction of fresh magmatic material into the vent, reflect the extent of dissolution reaction progress on the magmatic material and/or its alteration products. The results also provide insights into the role of such vent processes in the formation of high sulfidation-type ore deposits.

Key words: Volcanic crater lake – Fluid-mineral equilibria – Reaction path processes – Volcanic vent environments

Introduction

A two-year monitoring study of Ruapehu Crater Lake chemistry shows the chemistry to have evolved considerably since the volcano's more active periods in the 1970s, and indicates that open reaction path processes control the lake chemistry between phreatomagmatic eruptions.

Lake chemistry was previously studied by Giggenbach (1974) over the period December 1970–February 1973, a period which included the major phreatomagmatic events of 1971. Marked changes in lake chemistry subsequent to the eruptions were attributed to the introduction of fresh andesite into the vent/lake system. Since then, both the frequency and magnitude of the phreatic events have diminished, but the chemistry of the lake has continued to evolve to compositions quite distinct from those of the early 1970s.

In this paper we compare data collected between November 1988 and December 1990 to those from the early 1970s. Incorporating previously unpublished water and ejecta analyses obtained over the intervening period, we develop a reaction path model to explain the evolving state of the vent hydrothermal system and its influence on lake chemistry.

Lake history and behaviour

Except for a brief disappearance in 1945, the crater lake on Mt. Ruapehu has been a feature of the volcano since observations were first recorded in 1879. The lake disappeared in 1945 during a period of extrusive magmatic activity, but reestablished in 1946, and has since been the source of numerous phreatic and phreatomagmatic eruptions. Major eruptive events occurred in 1966, 1968, 1969, 1971, 1975, 1977, 1978, 1982 and 1988. Fresh pumiceous andesite was erupted in 1966, 1969, 1971, 1975 and 1977 (Cole and Nairn 1975; Nairn et al. 1979 and Wood in Healy et al. 1978), but juvenile material has only ever been a minor component of the ejecta, comprising for instance less than 5% of the 1969 eruption products (Healy et al. 1978). Eruptive activity waned in the 1980s, with major phreatic events recorded only in 1982 and 1988.

The lake is approximately oval in shape (Fig. 1), with an average diameter about 500 m, and an area of

Correspondence to: B. W. Christensen

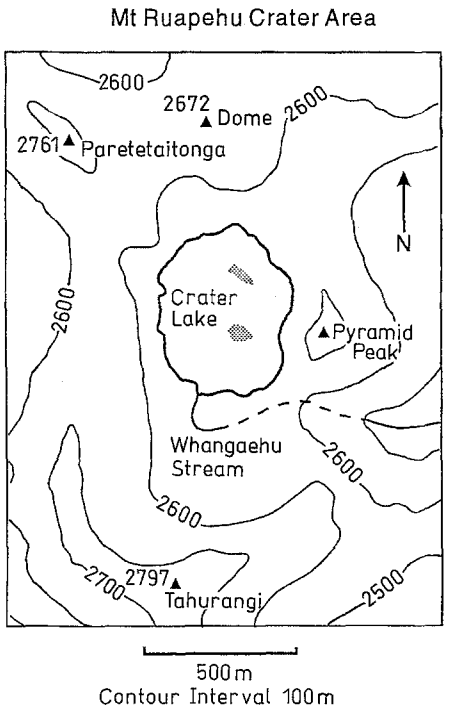

Fig. 1. Topographic sketch map of crater area. *Stippled areas* in the lake depict upwelling zones over the central and northern vents. All elevations are metres above sea level

about 0.2 km^2. The single outlet which forms the head waters of the Whangaehu Stream provides the main overflow discharge from the lake, although volumetrically minor internal leakage occurs, as indicated by spring discharges at a locality east of Pyramid Peak.

Bathymetry, and hence volume, of the lake have changed markedly through time. In 1965 the lake had a champagne glass bathymetric profile (Hurst and Dibble 1981), with a maximum depth over the central vent in excess of 300 m. By 1970 the depth of the central vent had decreased to 80 m (Irwin 1972), the result of both sedimentation and magma infilling of the neck of the glass (Glover in Healy et al. 1978). Maximum depth increased again to greater than 180 m between 1970 and 1982 (Nairn 1982), owing to the vent-clearing eruptions over this period. Recent bathymetric studies in 1991 (Christenson et al. 1992) found a maximum depth of about 134 m, and an estimated lake volume of ca. 9.0 million m^3.

As discussed by Hurst et al. (1991), the lake displays cyclic thermal and discharge behaviour, with temperature ranging between 10 and 60° C, and measured outflows from 0 to 500 l/s. During hot periods, convective upwellings are commonly observed over the deeper central vent region and in the north central portion of the lake (hereafter the northern vent). Heat input from

Table 1. Ruapehu Crater Lake Water Analysis: 1988–1990

Date	T° C	Outflow l/s	pH	Li	Na	K	Ca	Mg	Rb	Cs	Fe	Al	SiO_2	B	Cl	SO_4	NH_3	H_2S	F
14/11/88	9.0	150	0.71	0.36	297	104	760	340	0.69	0.05	418	1040	185	14.8	5466	16300	NA	NA	NA
9/12/88	13.7	300	0.73	0.37	302	106	748	340	0.66	0.05	420	1040	123	14.8	5531	16700	8.7	−1	234
16/12/88	14.0	100	0.73	0.37	303	107	742	350	0.66	0.05	438	1120	128	14.7	5478	16600	8.8	2	235
11/01/89	27.0	500	0.87	0.18	224	72	810	280	0.52	0.04	324	760	150	10.6	3983	12400	5.8	NA	163
24/01/89	32.2	420	0.77	1.10	305	101	618	380	0.78	0.20	448	1020	172	15.4	5727	15700	10.3	2	234
10/02/89	39.0	80	0.76	0.25	322	111	966	410	0.79	0.11	480	1080	124	15.4	5804	17200	7.3	<0.04	245
26/02/89	42.5	80	0.73	0.11	335	118	963	410	0.82	0.18	502	1160	125	16.0	5812	17800	NA	0.06	NA
21/03/89	32.0	−0.15	0.72	0.30	358	117	803	430	0.90	0.14	488	1240	164	17.2	6126	17400	8.3	<0.04	276
05/04/89	31.3	−0.06	0.73	0.26	360	114	937	430	0.89	0.14	492	1280	166	16.4	6164	16500	8.4	NA	278
11/05/89	25.0	−0.15	0.73	0.29	360	112	907	430	0.87	0.13	484	1160	158	17.2	6168	17900	NA	<0.04	252
14/06/89	25.0	−0.15	0.73	0.26	308	101	848	420	0.78	0.12	416	1060	172	14.5	5670	15250	9.4	<0.04	227
24/07/89	13.8	70	0.73	0.28	338	123	989	430	0.84	0.05	532	1260	163	16.8	6364	18700	9.6	<0.04	280
05/09/89	34.6	−0.25	0.78	0.25	389	139	989	440	0.89	0.15	468	1290	164	16.5	6731	18500	8.8	<0.04	315
19/10/89	25.0	−0.25	0.73	0.24	365	139	960	450	0.92	0.17	582	1320	147	16.2	6960	19700	9.1	NA	292
17/11/89	23.0	110	0.74	0.26	353	131	922	440	0.85	0.14	548	1320	153	15.8	6738	19300	8.4	0.12	280
11/12/89	22.0	11	0.73	0.25	374	128	952	430	0.85	0.13	544	1220	152	15.6	6641	18300	10.7	NA	274
11/01/89	27.0	400	0.70	0.10	348	118	882	380	0.75	0.11	508	1220	155	16.0	6158	18100	10.1	0.08	257
26/01/89	42.1	140	0.64	0.20	345	141	1006	401	0.84	0.13	495	1220	154	17.3	6551	20400	10.6	0.04	285
01/02/90	46.7	150	0.63	0.20	344	144	999	389	0.83	0.14	468	1360	152	16.9	6577	19400	8.6	0.04	279
16/02/90	46.2	140	0.70	0.24	362	151	946	398	0.85	0.17	520	1400	158	16.6	6630	19600	NA	NA	322
19/03/90	34.1	100	0.63	0.23	348	143	900	398	0.77	0.12	495	1280	170	14.6	6328	16600	9.1	NA	278
12/04/90	31.0	10	0.70	0.05	355	138	822	360	0.72	0.08	460	1370	188	17.2	6144	19200	NA	<0.04	272
10/05/90	25.8	35	0.69	0.05	350	144	772	361	0.75	0.09	442	1280	175	17.7	6526	20450	NA	<0.04	291
17/06/90	23.5	−0.20	0.73	0.16	345	149	888	355	0.73	0.04	434	1380	159	17.9	6650	19400	NA	0.04	310
20/07/90	20.0	−0.20	0.71	0.12	349	147	876	362	0.74	0.04	434	1360	164	17.3	6717	19500	NA	0.05	323
22/08/90	25.0	90	0.67	0.18	355	146	916	336	0.75	0.05	410	1320	180	16.8	6624	19700	NA	NA	312
11/09/90	30.0	30	0.71	0.12	349	147	876	362	0.74	0.04	416	1360	164	17.3	6717	19500	NA	NA	326
09/10/90	31.0	−0.40	0.63	0.17	387	153	928	368	0.77	0.04	456	1460	163	17.1	6933	19500	NA	NA	342
27/12/90	24.0	70	0.72	0.21	358	151	927	322	0.76	0.05	443	1440	135	18.4	6989	21400	NA	NA	343

All values as mg/l; NA stands for not analysed. Negative values for outflow indicate metres below overflow level

Table 2. Trace element data

	Crater Lake 1971–1973	Crater Lake 26/1/90	White Island Fumarole #3 2/12/88[1]
Br	16.8–18.4	10.0	13.1
Zn	2.8–4.8	2.16	0.375
As	0.2–3.3	1.6	1.2
Sb	NA	0.0045	0.0035
Cr	0.3–1.5	NA	0.120
Pb	0.4–0.9	0.96	0.081
Ti	0.2–1.0	NA	29.000
Ni	0.2–0.9	1.1	0.048
Cu	0.1–0.2	0.03	0.027
Ag	NA	0.0005	0.0002
Au	NA	<0.00005	0.00033
pH	1.18–1.78	0.64	NA
T (° C)	28–53	42	354

[1] Taken with Ti sampling train, hence the high Ti values
1970s data taken from Giggenbach (1974); fumarolic data for White Island #3. All values mg/l

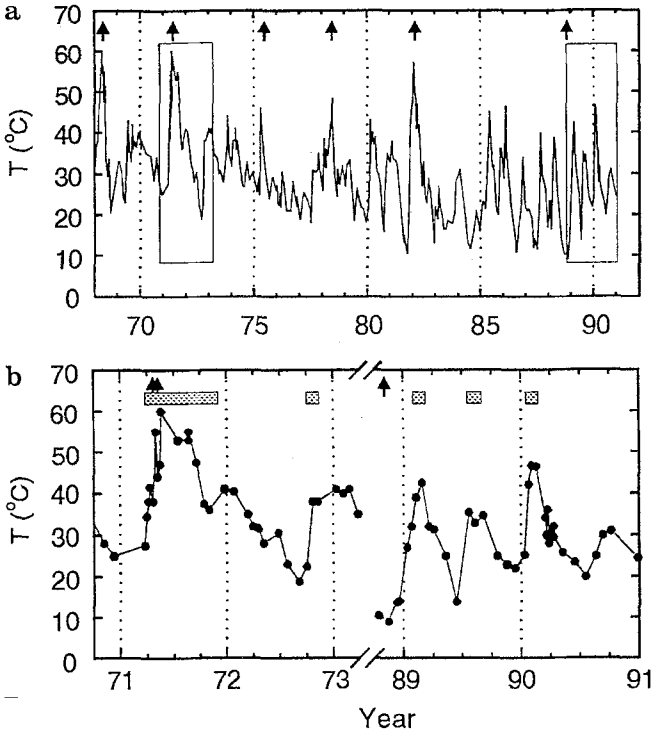

Fig. 2 a, b. Outlet temperature. **a** Comprehensive plot of the period 1968–1991. *Arrows* represent major phreatic or phreatomagmatic eruptions, and boxes denote periods of detailed studies in the 1970s and 1980s. **b** Expanded scale plots. *Arrows* again represent major eruptive events and *stippled boxes* denote periods of hydrothermal activity

the northern vent appears to be minor in comparison to that from the central vent, as the lake continues to cool when it alone is active. When both vents are shut, the lake changes from its characteristic grey to a blue-green colour, owing to the settling of suspended load.

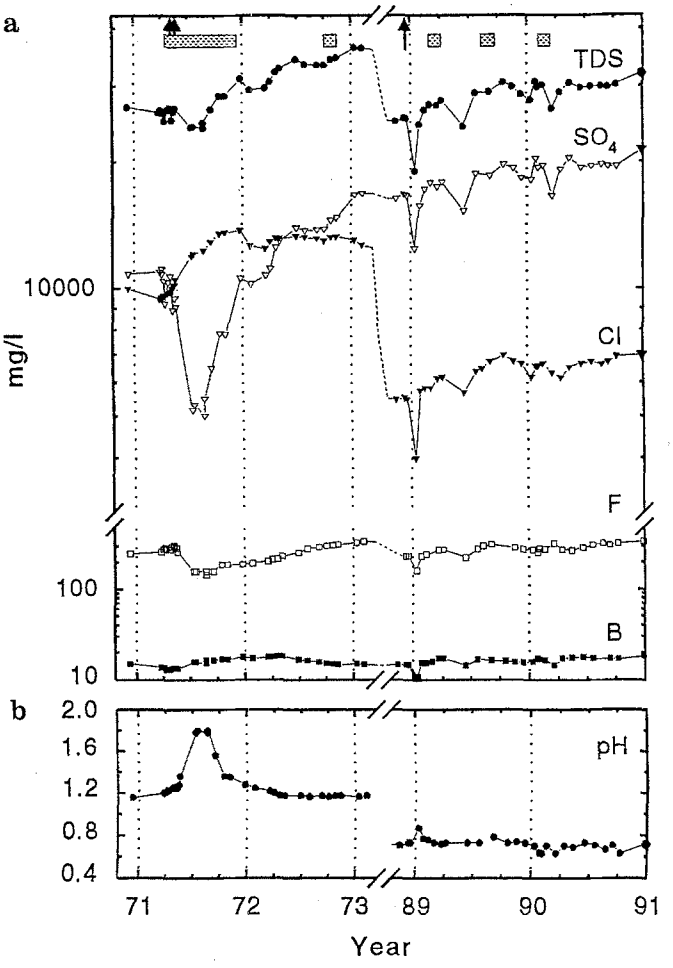

Fig. 3. a Crater Lake anion concentration (mg/kg). *Arrows* represent major eruptive events, *stippled boxes* denote periods of hydrothermal activity. **b** Crater Lake pH (20° C)

Data

Temperature and chemical data collected over the period November 1988 to December 1990 are listed in Table 1; all measurements and samples listed are from the outlet channel. Temperatures were measured by thermocouple and/or maximum reading Hg in glass thermometer, and outflows were estimated from channel dimension and flow velocity measurements.

Three samples were collected for each chemical analysis, including a 500 ml sample for pH and anion analysis, a 100 ml (0.45 μm) filtered sample for cation analysis, and a 250 ml air-free sample for reduced S analysis. The filtered suspension was, wherever possible, retained for X-ray diffraction (XRD) analysis.

Cations and silica were analysed by atomic absorption spectrophotometry (AA), SO_4, B and H_2S by spectrophotometric methods, Cl by potentiometry, and NH_3 and F were measured by specific ion electrodes. The single trace element analysis reported in Table 2 was obtained by inductively coupled plasma mass spectrometry and graphite furnace AA.

Ejecta and suspension samples were examined under binocular and petrographic microscope, and fur-

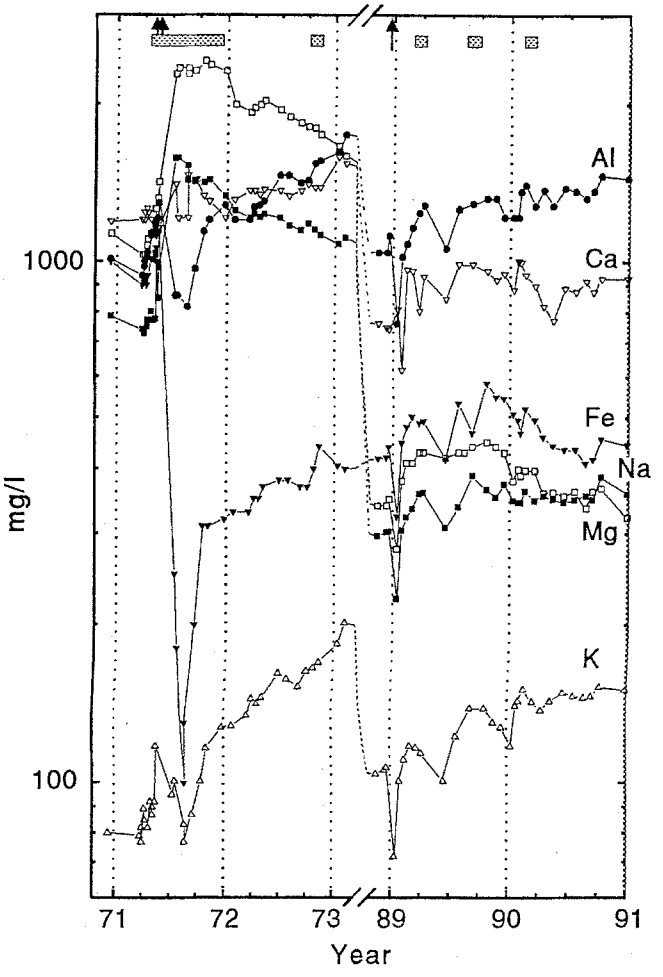

Fig. 4. Crater Lake cation concentrations (mg/kg). *Arrows* represent major eruptive events, *stippled boxes* denote periods of hydrothermal activity

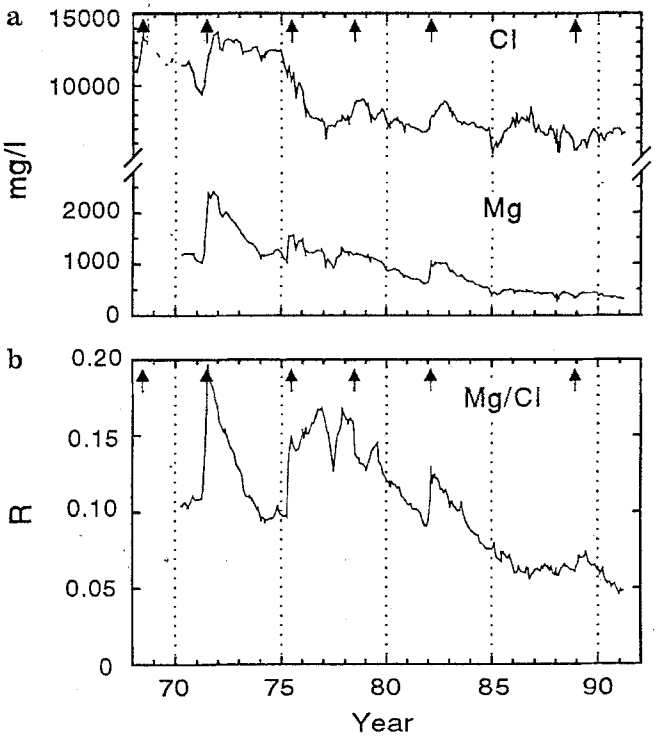

Fig. 5 a,b. Time series chemical data for the period 1968–1991. **a** Mg and Cl; **b** Mg/Cl ratio. *Arrows* denote major eruptive events. (Unpublished DSIR data)

ther analysed where necessary by X-ray diffraction, infra-red spectroscopy and scanning electron microscope-energy dispersive X-ray analysis (SEM-EDX).

Lake temperatures and chemistry

Outlet temperatures for the period 1968 to 1991 are plotted in Fig. 2a, with expanded time scales covering the two sampling periods in Fig. 2b. Only major phreatic eruptions are indicated in Fig. 2a, whereas both major events (arrows) and periods of hydrothermal activity (stipped boxes) are indicated in the expanded plots.

The data reflect both the periodic behaviour of heat input into the lake, and the obvious relationship between heating cycles and the larger eruptive events. Lake heating is typically very rapid, whereas cooling periods range between 0.5 to 1.5 year's duration. The major eruptions (especially those in 1971 and 1975) occur near the peaks of their respective heating cycles, and have longer cooling periods than the other cycles. Such slower cooling may be the result of either the high level emplacement of magma into the upper vent zone, eruption-induced enhancement of permeability in the vent region, or both.

The 8 December, 1988 block eruption was different to those of the 1970s in that it occurred when the lake was at a low temperature. This eruption ended a three-month period over which there was no observed convection, and the lake reached the lowest temperature ever recorded (9° C). Ejecta petrology and lake compositional variations (discussed below) indicate that this was a vent-clearing eruption (Christenson, in press) which introduced no juvenile magmatic material, but reestablished heat flow into the lake and enhanced the recirculation of lake water into the upper portion of the vent.

Complete chemical analyses of the lake waters from the 1971–1973 and 1988–190 sampling periods are compared in Figs. 3 and 4. The 1988 total dissolved solid contents (TDS) are not substantially different from those recorded in the 1970s (Fig. 3a), but this is because the dilution in Cl and F since the 1970s is offset by increases in SO_4, which by the end of 1990 stood at the highest levels ever recorded for Crater Lake.

Short-term variations associated with the 1971 period of activity included a near 50% increase in TDS over the two years following the 1971 eruptions (Fig. 3a). Whereas Cl levels increased sharply subsequent to the eruptions, this trend was offset by an equally abrupt decline in SO_4 concentrations. SO_4 values rapidly recovered to pre-eruption levels within six months of the eruptions and continued to increase, nearly doubling in concentration by early 1973. Variations in B concentration were similar to those of Cl except during

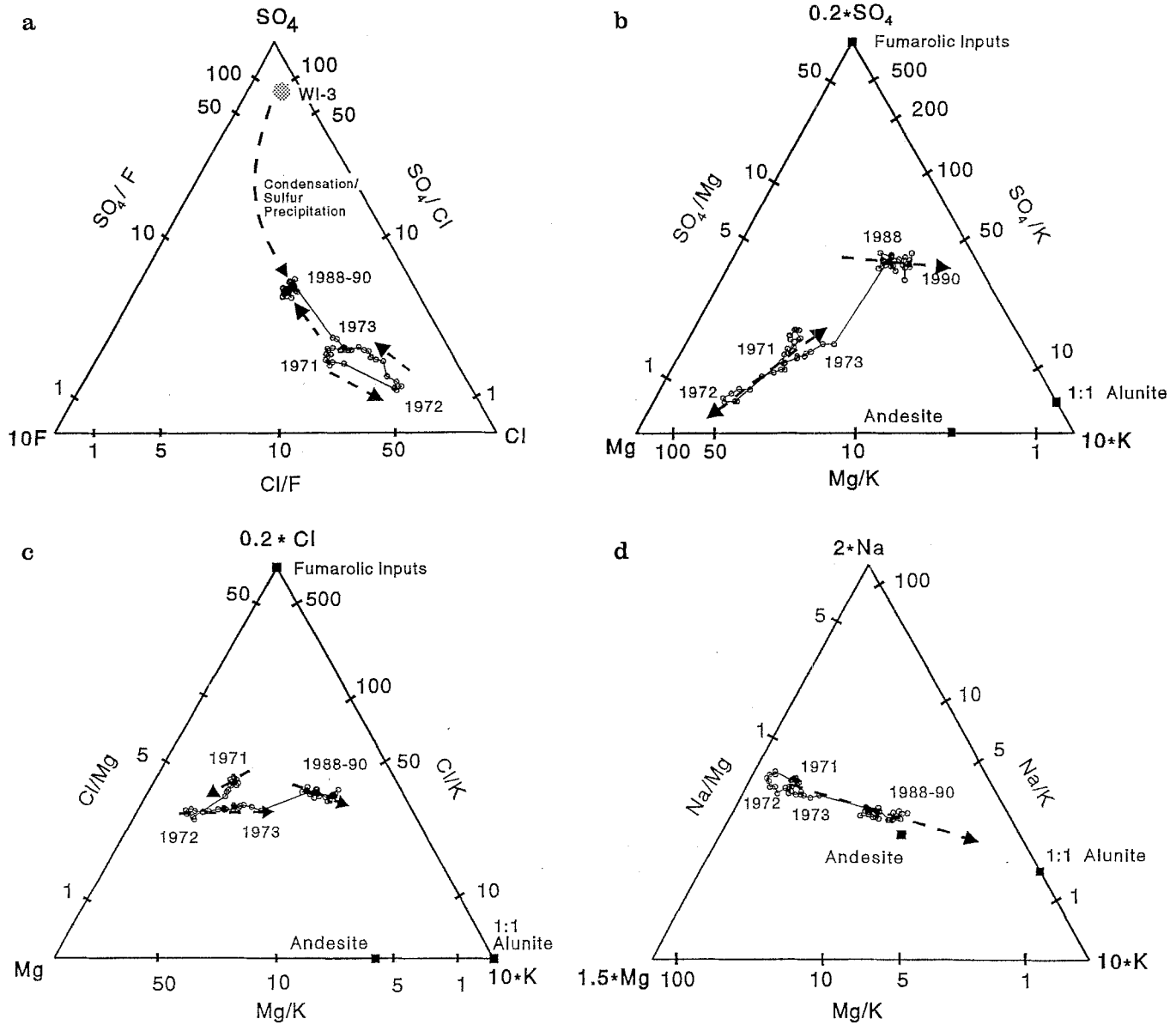

Fig. 6 a–d. Ternary plots of selected solute components. *Heavy dashed arrows* depict time series trends for the components: **a** SO_4-F-Cl; **b** SO_4-Mg-K; **c** Cl-Mg-K and **d** Na-Mg-K

the post eruptive recovery period in 1972 when the Cl/B ratio persistently increased.

In contrast, there were no significant chemical changes in anion concentrations associated with the 1988 phreatic event, only gradual increases in SO_4, and to a lesser extent Cl, since that eruption. The single, abrupt decline in all anion (and cation) concentrations in early 1989 is due to dilution by surface runoff waters after a period of heavy rain.

The pH rapidly increased by more than half a unit after the 1971 eruptions (Fig. 3b) but returned to pre-eruption levels by mid-1972, whereas pH was seemingly unaffected by the 1988 eruption. It is notable, however, that the 1988–1990 baseline values are some one-half unit more acid than those of the 1970s.

Of the cations plotted in Fig. 4, Fe and Al show the most immediate post-1971 eruption changes, abruptly declining by factors of 10 and 2 respectively. Both reach sharply defined minima within three months of the eruptions, before establishing long-term recoveries to pre-eruption levels. On the other hand, Mg and Na concentrations doubled within a month of the May 1971 eruptions, but declined over the subsequent 18 months. K concentrations also abruptly increased by ca. 20% after the May eruptions, but returned to pre-eruption levels during the subsequent three months. From September 1971, however, K concentrations began to increase, and by 1973 had increased by a factor of ca. 2.5.

As for Cl, cation concentrations in the 1980s are generally lower than those in the 1970s. Mg, which increased only slightly after the 1988 eruption, subsequently resumed its long-term trend of declining concentration. K and Al, on the other hand, steadily in-

Table 3. Alteration phases in vent ejecta

Sample	Cristobalite	Sulfur	Pyrite	Alunite	Anhydrite	Amorph. Silica	Other/Comments
RU-7	×	7.1%	×	×	×		NaCl, KCl in laminated sediment/breccia
RU-8	×	0.93%			×	×	Porous, vesicular sediment, vesicles to 2 mm diameter
RU-9	×	abund.	×	×	×		Vesicular breccia with abundant sulphur globs
RU-10	×	0.64%	×		×	×	Fine-grain vesicular sediment
RU-11			×				Coarse breccia
RU-20	×				×		18 kg boulder, cavity fillings of alteration minerals
RU-28		×					Lithic crystal ash with abundant sulphur spherules
RU-30	×			×	×		Indurated bottom sediment
RU-32		×			×		V. fine ash with anhydrite crystals + sulphur spherules
P536	×	×	×	×	×		Halite on altered andesite
P537			×		×		Hematite on pyritic, coarse lake sediment
P539A	×	×			×		Medium-grained sediment
P539B							Fresh andesite with trydimite in cavities
RU-44	×	×	×	×	×		Sulphurous andesitic tephra, trace pyrophylite
RU-45	×			×	×		Distal ash unit, trace pyrophyllite
RU-51	×	×	×	×			<63 μ fraction of tephra, with sulphur spherules and trace of trydimite
SP12-88	×	×				×	Opal C-T
SP01-89	×					×	Opal C-T, trace gypsum
SP01-90	×					×	Opal C-T
SP02-90	×					×	Opal C-T, gypsum
SP02-91	×					×	Opal C-T

RU1-32 Ejecta from 8/ 5/71 eruption
P series Ejecta from 27/ 4/75 eruption
RU44-45 Ejecta from 2/11/77 eruption
RU51 Ejecta from 20/11/81 eruption
SP series Suspended sediment

creased in concentration over the two years to December 1990, whereas Ca and notably Fe showed no consistent trends over this period.

Trace element data from January 1990 (Table 2) are comparable to those from the 1970s (Giggenbach 1974) and to fumarolic condensates from White Island (Table 2). Only Br and possibly Cu reflect the dilution evident in the major constituents between the 1970s and 1980s, although there is some uncertainly that the variation in Cu concentrations relates to the differing detection limits of the respective analytical methods. All other data fall close to or within the previous recorded ranges of concentration.

Complete lake water analyses were not obtained between 1973 and 1988; samples collected during this time were analysed for only Mg and Cl ions, as these species were deemed sufficiently diagnostic of water–magma interaction (Giggenbach 1974; Giggenbach and Glover 1975). Superimposed on the long-term dilution trend between 1970 and 1990 are a number of episodes where the concentrations of both Mg and Cl abruptly increased (Fig. 5a), each corresponding to a period of eruptive activity. Similarly, the Mg/Cl ratio shows a long-term decline (Fig. 5b), with abrupt reversals again correlating to eruptive activity, particularly the 1971, 1975, 1982 and to a lesser extent 1988 events.

Mineralogy of ejecta and suspension samples

Ballistic ejecta from the larger eruptions of the last 20 years consist of both juvenile and accessory components. Scoriaceous pumice bombs, some with breadcrust structure, were ejected during the 1971, 1975 and 1977 eruptions, proving the rise of magma into the vent at these times. Accessory lithic ejecta include lake bed sediments, andesite breccias, and various andesitic lavas (Nairn et al. 1979). The sediments, which range from fine silts to coarse breccias, typically include variably altered andesitic lithics incorporated in fine-grained muds.

Ejecta alteration mineralogy is summarised in Table 3; the most abundant phases are low-temperature silica polymorphs (cristobalite and opal CT), sulfates (anhydrite, gypsum, and alunite group), pyrite and native sulfur. The alunite phase most often identified is natroalunite, based mainly on XRD cell dimensions; Giggenbach (1974) reported a natroalunite analysis from a suspension sample with a stoichiometry of:

$$(Na_{0.56}, K_{0.44})\,Al_3(SO_4)_2(OH)_6.$$

Pyrite and anhydrite are ubiquitous, occurring as vug fillings and as dispersed phase in the ejected sediments, whereas microcrystalline pyrite also occurs with opaline silica in floating mats of spongy sulfur. Hematite,

found coexisting with anhydrite, is indicative of the locally oxidising conditions in the alteration environment. Although clay phases are not common in the ejecta, minor amounts of kaolinite or pyrophyllite have been identified in three ejecta samples. The occurrence of fracture fillings of halite and sylvite in ejecta sample RU-7, in quantities easily observable to the naked eye, point to the existence of highly concentrated brines in the vent.

Evidence of high vent temperatures has been found in the form of partly remelted andesitic tuff, and ejecta containing phases belonging to the pyroxene hornfels and sanidinite metamorphic facies (Nairn et al. 1979). For example, one lake sediment block ejected in the 1975 eruption was found to be completely recrystallised to an assemblage: plagioclase + magnetite + hedenbergite + hypersthene + trydimite whereas others contain, in addition to the above assemblage, sanidine, pseudobrookite, cordierite and the rare silicate osumilite. These assemblages, indicating local temperatures in excess of 750° C, clearly reflect vapour phase or contact metamorphic origins within the vent associated with high-level magma emplacement.

A number of well-indurated sediment samples are vesiculated, containing narrow tubes and channels up to 1 cm long which may have served as passageways for ascending vent gases. In some cases, the passages were lined or infilled with elemental S, which likely precipitated in situ from the passing gases; on ejection from the vent in 1971, liquid S was observed to 'sweat' from such samples, being pushed out of the pores and vesicles by flashing pore waters (Giggenbach 1974).

Suspended sediments filtered from the lake waters during the 1988–1990 sampling period were found to consist mainly of opal CT with trace amounts of gypsum (Table 3), which contrasts to occurrences in the 1970s of these phases plus natroalunite in the suspension (Giggenbach 1974). It is important to note that the suspensions are precipitates which form directly in the lake where the occurrence of gypsum indicates formation temperatures of less than about 56° C (Blount and Dickson 1973). Dispersed S was identified in the suspension only after the December 1988 eruption, although it is usually present as surface scum when the vents are open and the lake is actively convecting.

Sources and sinks of solute constituents

There are two primary sources of the dissolved constituents in Ruapehu Crater Lake: the anionic components originate principally as volatiles which decouple from the underlying magma and stream upward through the vent/lake system; cationic constituents derive dominantly from dissolution of andesitic material, although trace levels of metal halide constituents are also carried by high-temperature fumarolic gases (e.g. Gemmel 1987; Symonds et al. 1987; and Table 2). As degassing proceeds, the volatile species (consisting mainly of CO_2, SO_2, H_2S, HCl, HF, HBO_2, N_2, H_2, CO, NH_3 and metal halides) ascend toward the vent. In the single phase vapour P-T region, sublimation reactions precipitate halide and sulfide solid phases on conduit walls. As temperatures decrease along the conduit to the saturation point for liquid water, the more soluble and/or reactive constituents, i.e. the metal halides, HCl, HF, HBO_2, NH_3, SO_2, H_2S, and to a lesser extent H_2, react with and/or fractionate into the aqueous phase forming an acidic condensate solution. The remaining, less soluble and/or less reactive constituents (e.g. CO_2) pass through the vent–lake system to the atmosphere.

Where magma is emplaced at high levels in the vent, in situ degassing results in the formation of a concentrated brine phase adjacent to the magma, with quantity and salinity of the brine being dependent on the absolute pressure controlling the degassing process (e.g. Burnham 1979; Pitzer and Pabalan 1986). Within 100 m of the lake floor, the maximum confining pressures would be about 300 bars, resulting in a brine which is likely to be saturated with respect to NaCl/KCl, but having an exceedingly small brine/vapour mass ratio. It is possible that such brine segregations could be expelled into the lake during eruptive episodes, but the overall impact on lake chemistry is likely to be negligible.

Factors contributing to changes in the concentration of soluble fumarolic species in the lake include the general level of magmatic degassing as well as dilution and evaporation processes of the lake itself. Relative variations among the fumarolic constituents may, on the other hand, result from temperature cycling in the fumarolic conduits, as noted for fumarolic discharges at White Island (Giggenbach and Sheppard 1989), or by the formation of secondary minerals in the saturated vent/lake environment.

Although trace amounts of metals are likely to be carried by vapours entering the two-phase liquid vapour zone (Table 2; Gemmell 1987; Symonds et al. 1987), the bulk of non-volatile solutes in the lake water (i.e. the alkali, alkaline earth and transition metals) originate from dissolution of the host magmatic material. In the case of Ruapehu, the lavas and pyroclastics are of andesitic composition (Table 4). In the absence of secondary chemical processes, there would be little or no variation in non-volatile solutes through time, and the constituents would be present in approximately 'andesitic' proportions. However, large relative variations in solute concentrations (Giggenbach 1974), particularly during the 1971 period of eruptive activity, indicate a more complex situation (Figs. 3, 4). Coupled with the occurrence of alteration minerals in vent ejecta, these changes indicate the existence of heterogeneous equilibrium processes actively operating in the vent.

Solutes not entering into fluid-mineral equilibrium reactions include Mg, Cl, Mn, and possibly B (Giggenbach 1974) whereas those affected by observed secondary minerals (Table 3) include Na, K, Al, Ca, Fe, S and H. Hydrogen ions are consumed in hydrolysis reactions during dissolution of the host andesite oxides and/or secondary minerals via reactions such as:

Table 4. Analyses of Ruapehu juvenile andesitic ejecta used in the modelling

	1969 (P38489)	1971 Average Andesite	1971 Standard Deviation
SiO_2	61.50	59.73	0.73
TiO_2	0.74	0.65	0.13
Al_2O_3	15.10	16.28	0.16
Fe_2O_3	1.75	2.10	0.15
FeO	4.55	4.64	0.43
MnO	0.09	0.09	0.22
MgO	3.50	4.67	0.07
CaO	6.40	7.23	0.02
Na_2O	3.43	3.32	0.02
K_2O	2.25	1.41	0.01
P_2O_5	0.23	0.16	0.01
H_2O+	0.35	0.24	0.10
H_2O-	0.05	0.02	0.01
Total	99.94	100.54	
Mn	700		
Cu	39		
Zn	60		
Pb	19		
Ba	467		

P38489 is an andesitic pumice bomb, ejected 22 June 1969 (Healy et al. 1978). Average 1971 values derive from four scoria bombs ejected during the 8 May 1971 eruption (Nairn et al. 1979)

$$M_{2/z}O + zH^+ = M^{z+} + H_2O$$

where M represents an oxidic rock component. Although F-bearing minerals have not been identified in any ejecta, variations in aqueous F concentrations suggest that a mineralogical sink probably does exist for this component (perhaps fluorite or fluor-apatite, discussed below). Similarly, the behaviour of certain trace metals (such as Ni, Pb or possibly Cu) is indicative of secondary equilibrium processes.

There are three groups of reactants in the vent hydrothermal environment, i.e. the volatile species, unaltered andesitic material, and earlier-formed reaction products, all of which leave distinctive signatures on the fluid. The effect of each reactant on lake composition over the last 20 years is obtained from their normalised relationships through time (Figs. 6a–d).

The three major volatile components in the lake water, i.e., Cl, SO_4 and F, plot in normalised positions distinct from that of the inferred magmatic vapour composition (e.g. White Island fumarole #3; Fig. 6a), owing principally to the precipitation of elemental sulfur in the vent-lake environment. Eruption-induced changes in the lake water composition include the marked relative increase in Cl subsequent to the 1971 eruptions, and the rapid recovery to pre-eruption values by 1973. The increase in Cl, in absolute terms, is easily explained by increased introduction of fumarolic HCl gas into the lake following the eruption. However, the absolute declines in F and especially SO_4 cannot be explained by fumarolic processes, but rather by secondary process(es).

The concentration of SO_4, the dominant S species in the lake (Webster 1989), is a function of not only the amount of fumarolic gas entering the lake but also of sulfur speciation and SO_4 precipitation and re-dissolution processes. Fumarolic sulfur inputs are dominated by SO_2 and H_2S, and once inroduced into an aqueous environment, a series of reactions may ensue. For example, SO_2 dissolves in water to form sulfurous acid, which readily disproportionates to H_2SO_4 and H_2S (Kiyosu and Kurahashi 1983). At the same time, reactions between SO_2 and H_2S, lead to the formation of elemental S (Mizutani and Sugiura 1966), and polythionates (Takano and Watanuki 1989). The polythionates, however, can be regarded largely as quantitatively minor, transient species which ultimately break down to form S° and SO_4 at elevated temperatures. Further, since the lake is open to atmospheric oxygen, any H_2S remaining after the above reactions might be expected to oxidise to S° which, along with all other intermediate oxidation states, is subject to further oxidation by bacterial action. Since SO_4 is the stable reaction end-product in each of these processes, it becomes necessary to consider heterogeneous equilibria involving this species (i.e. the formation of alunite or anhydrite) to account for its dramatic consumption following the 1971 eruptions.

The compositional trend subsequent to the May 1971 eruptions (Fig. 6a), can therefore be explained in terms of net Cl additon by increased fumarolic inputs, but removal of F and SO_4 through mineral precipitation. Recovery to pre-eruption ratios requires either changes in the composition of the fumarolic inputs, perhaps through liquid phase scrubbing of halogen constituents from the gas stream along two-phase (i.e. vapour-liquid) conduits, dissolution of previously-formed SO_4 mineral phases, or both.

Sulfate mineral dissolution is indicated from the relative changes in Mg, SO_4 and K in Fig. 6b. The increasing in Mg subsequent to the May 1971 eruptions is consistent with dissolution of andesite, as described by Giggenbach (1974), whereas the trend away from the andesitic composition during this time is indicative of K uptake in the formation of alunite. Between late 1971 and 1973, however, this trend reversed as SO_4 was contributed by both previously formed alunite and fumarolic inputs. The subtle change in the pathway trajectory since 1988 also suggests an increased proportion of alunite SO_4 in the lake since 1973.

There were abrupt post-eruption increases in the Mg/Cl and Mg/K ratios (Fig. 6c), followed by prolonged declines in both, similar to the K-Mg-SO_4 trend. The different trajectories of the pre- and post-eruption trends are due to: (1) precipitation and then dissolution of alunite; and (2) initial dissolution of andesite (Mg enrichment in lake water) followed by sustained addition of HCl into the lake.

Variations between Na-K-Mg in Fig. 6d are consistent with the above trends and conclusions regarding Mg behaviour. The trend since late 1971 also shows, however, that sodium does not behave conservatively in the vent/lake environment, but rather is controlled

by the sodic component of an approximately 1:1 Na-K alunite phase (i.e. natroalunite).

Water–rock interaction in the vent complex

Compositional variations in Crater Lake immediately after the 1971 eruptions were clearly related to the dissolution of andesite. Some dissolution may have occurred when near-incandescent ash and lake water mix, but this process alone is not supported by the persistent, long-term changes affecting the water composition days or weeks after an eruption. It is more likely that the reactions take place within the vent, where cooling magmatic material reacts with hot, acidic solutions (lake water and/or fumarolic condensate). In this situation, vent-clearing eruptions expel previously reacted fluid into the lake and enhance permeability in the vent zone, thus accelerating further convection and reaction. This is supported by the fact that there is little direct evidence of andesite alteration within the lake itself, a feature also noted by Giggenbach (1974). Andesite blocks and boulders on the lake shore and in the outlet channel do not show any evidence of weathering or alteration, nor do juvenile pumiceous bombs and andesitic glass foam found floating in the lake after phreatomagmatic eruptive events (Wood 1975).

The occurrence of halite and sylvite in ejecta which otherwise lack high temperature (i.e. vapour phase) alteration points to the localised development of highly concentrated fluids in the vent zone. As mentioned above, brines may form through magmatic degassing, but the volumes generated in this way are unlikely to form a pervasive brine phase in the vent. It is more likely that halide salts found on fracture surfaces of laminated vent sediments (e.g. RU-7, Table 3) precipitated during localised evaporation (i.e. boiling) of resident vent fluids. Boiling is expected to be a common occurrence in the vent, resulting from both eruption-induced pressure transients and cyclic variations in heat flow.

The abrupt increase in conservative species (such as Mg and Cl) noted in the lake even one day after each of the 1971 eruptions (Giggenbach 1974) are most easily explained by the physical expulsion into the lake of previously formed brine fluids and earlier dissolution products. Subsequent to the eruption, convective circulation of lake water through fresh andesite in the fractured vent zone would promote both further flushing of earlier-formed brines and further andesite dissolution.

It is evident from the 20-year record of outlet Mg and Cl contents (Fig. 6a) and Mg/Cl ratios (Fig. 6b) that such processes have continued since the major eruptions of 1971. Superimposed on the general trend of declining Mg concentrations over this period are a number of abrupt reversals, the larger of which correspond to recognised eruptions of juvenile ash (i.e. 1971, 1975 and 1977). Several of the smaller perturbations in the Mg/Cl ratio, including those in 1976, 1982 and even 1988, are associated with only hydrothermal eruptions which apparently only clear the vent of previously reacted fluids.

Recent trends indicating dissolution of previously formed hydrothermal phases are less ambiguous in their origins. The enrichment trends indicating natroalunite dissolution have continued through periods lacking eruptive activity of any kind, and as such indicate steady state discharge into the lake from lake-floor hot springs.

Convective recirculation of lake water in the vent zone

Through a heat and mass study of the lake, Hurst et al. (1991) determined that the lake was receiving more heat than could be accounted for by the mass of water entering the lake as steam. To account for this discrepancy, they suggested that a stable heat pipe operates between the single-phase region surrounding the magma body and the overlying saturated two-phase zone in the fumarolic conduit. Heat pipes, which have been suggested to exist in a number of vapour-dominated geothermal systems (e.g. McGuinness and Pruess 1987; Ingebritsen and Sorey 1988), have three basic requirements for their existence (Eastman 1968). Along with a heat source, the cells need an effective heat sink and a readily condensable transporting medium. In the case of Ruapehu, Hurst et al. (1991) suggest that magmatic steam condenses to water near the top of the vent, releases its latent heat, and then drains under gravity back down to the heat source. Non-condensable volatiles must pass through the system, lest the efficiency of the heat pipe be compromised through a vertical increase in gas pressures (McKibben and Pruess 1988). In this respect, the feature operating on Ruapehu would be better referred to as a leaking heat pipe.

Although Hurst et al. (1991) do not discuss a heat dispersal mechanism in the heat sink area, some process must operate to remove heat from the condensation zone or the heat sink would degrade and the heat pipe would cease to operate.

A heat pipe model which includes circulation of lake water into the upper portion of the vent can explain both the chemical variations and heat flow characteristics of the lake (Fig. 7). Here a convecting and degassing magma body is portrayed underlying the central vent, and although the dimensions and absolute position of the magma body are largely schematic, they reliably represent an average view of the very dynamic magmatic conduit system. The magma body and immediately adjacent vent region is enclosed by single-phase vapour. This region is enclosed by a two-phase liquid-vapour zone which, in turn, is enveloped by a single-phase liquid (i.e. water). Condensation of magmatic volatiles occurs over the entire length of the two-phase zone, which is portrayed here as extending to the lake floor. The northern vent conduit, which occurs along the trace of a ring fracture (visible in photographs of the lava lake taken in 1945; Gregg 1960), is portrayed here as containing a two-phase fluid.

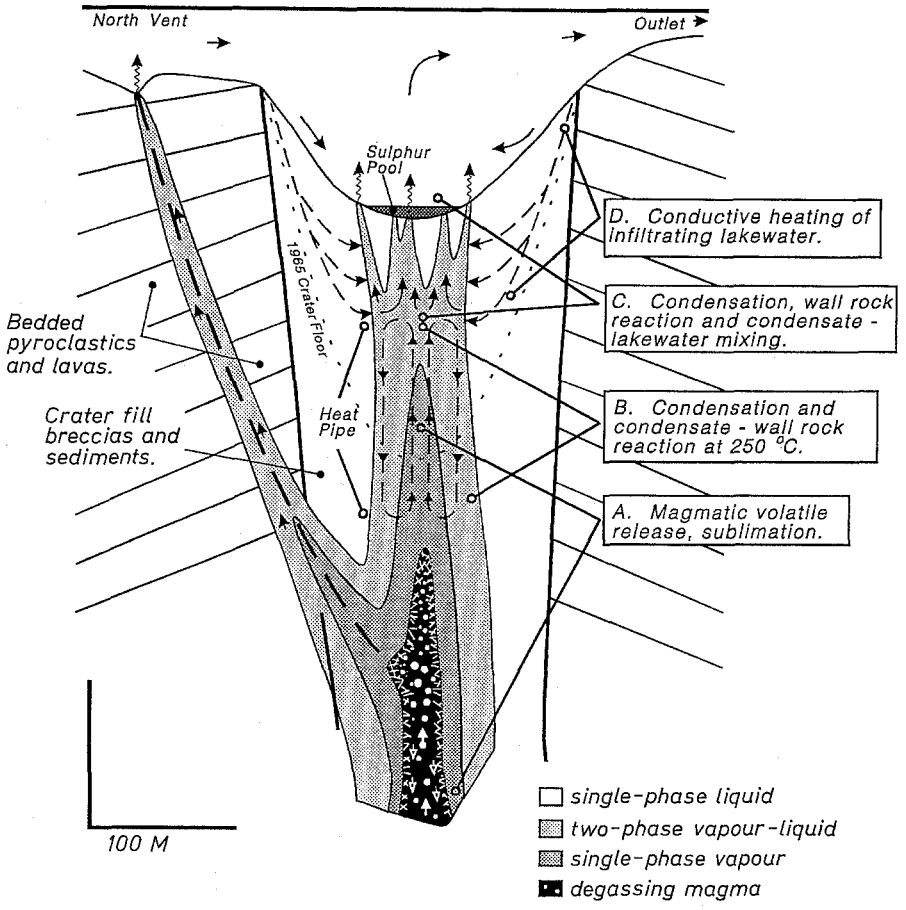

Fig. 7. Physical model of vent system. *Heavy near-vertical lines* denote the boundaries of the central vent, and the *dotted line* in the central vent complex represents the approximate bathymetric profile in 1965. Magmatic volatiles (including CO_2, SO_2, H_2S, HCl, HF and trace metals) released from the convecting magma column form sublimates along the negative thermal gradient in the single-phase vapour region denoted 'A'. In region 'B', vapour condensation at 250° C precipitates elemental S at pH 0.8, scrubs metal species into the liquid phase, and promotes hydrolysis reactions with andesite-forming silica, pyrite, anhydrite, alunite, covellite and pyrophyllite. Condensation and condensate–lake water mixing occurs in region 'C', leading to the precipitation of further sulfur, as well as pyrite, silica, gold, and covellite. Conductive heating of descending lake water occurs along region 'D', precipitating anhydrite above 250° C

Circulation of lake water into the vent zone is limited to the central vent fill complex. The vent is filled largely with eruption rubble and is assumed to be of high permeability relative to adjacent rocks which consist largely of interbedded lavas and andesitic tephras. The limited permeability along bedding planes is exemplified by the single issuance of hot springs referred to above. A pool of molten sulfur (located February 1991; Christenson, in press 1993) is portrayed here overlying fumarolic and hot spring vents.

The boiling-point temperature at 134 m depth is ca. 196° C at a confining pressure of 14.3 bars, given an average water column density of the lake during non-convective periods of about 1.02 g/cc (at 20° C). Although the additional confining pressure imposed by a 10 m deep pool of molten sulfur (at 2.0 g/cc) raises this temperature to only 202° C, confining pressures deeper in the vent are likely to exceed hydrostatic from time to time owing to viscosity variations of sulfur with temperature and mineralogic sealing of conduits. Evidence of intermittent overpressuring is the large phreatic eruption of 1988 which occurred during a period of low lake temperature.

Lake water is shown in Fig. 7 as penetrating into the upper vent complex along the steeply dipping boundary structures of the vent complex. Conductively heated as it descends, the water ultimately reaches the two-phase zone where it mixes and equilibrates with ascending fumarolic components. The heat pipe, operating as a discreet cell beneath the mass of convecting lake water, transfers heat and non-condensable components to the overlying lake water via a complex network of fractures.

This model has several distinctive reaction environments for vent fluids, as summarised in regions A–D in Fig. 7 and discussed below. However, the hydrothermal environment in the vent will be very sensitive to heat inputs, with single-phase vapour regions, for example, increasing in size during magmatic eruption events and decreasing during quiescent interludes. Expansion and collapse of the respective environments result in the overprinting of reaction pathways, changing P-T-X conditions and increasing the number of reactant species. Owing to the complexity of the processes involved, in the remaining sections we adopt a computer-modelling approach to assist in identifying the primary chemical processes affecting lake composition.

Chemical modelling of vent and lake fluids

Using appropriate end-member reactants, it is possible to model the chemical interactions in the vent and lake system thermodynamically. The model results may then be compared to lake water compositional trends, observed altertion assemblages and eruptive history in

order to assist in identifying the dominant hydrothermal processes at work in the vent/lake system.

Two computer codes were utilised in this treatment. SOLVEQ (Reed 1982) was used to calculate the speciation and saturation indices of alteration minerals in the lake water, and the reaction path code CHILLER (Reed 1982; Reed and Spycher 1984) was used to model equilibrium reactions between condensed fumarolic species, unaltered Ruapehu andesite and lake water.

Two design limitations of the code CHILLER hinder rigorous application of the reaction path model to the perceived vent system at Ruapehu. First, the database's upper temperature limit of 330° C precludes modelling processes above this temperature. Second, the code cannot be conveniently applied to problems involving the titration of vapour phase (i.e. fumarolic) constituents through open, two-phase (i.e. liquid–vapour) environments. Therefore we have limited our modelling to reactions involving a single (i.e. condensed) liquid phase at temperatures below 330° C.

However, these limitations do not seriously affect the validity of this computational approach aimed at identifying processes affecting lake chemistry. The chemical reactions involving non-volatile species which have the greatest effect on lake composition occur in the liquid phase. Therefore the maximum temperature in this reaction environment will be regulated by the PTX boiling-point constraints of the resident solution. Ignoring the relatively small additions from vapour phase sublimation processes, sustained temperatures above the boiling curve will result in a 'dry' reaction environment, wherein reactions involving the host rocks are largely isochemical and probably very slow.

If we somewhat arbitrarily impose a 200 m limit on the maximum depth of liquid phase recirculation in the system (as portrayed in Fig. 7), the hydrostatically controlled temperatures within this portion of the vent would range between ca. 190 and 250° C, well within the limits of the code.

The consequences of using precondensed fumarolic inputs in the modelling, however, are not easily dismissed as they relate to the fundamental differences between open and closed reaction systems. For example, a two-phase conduit which has differential movement of vapour past a less mobile liquid phase must be regarded as an open system, given that the partial pressures of the main hydrolysis-promoting agents in this environment (SO_2 and HCl) will remain more or less constant in the liquid phase. In terms of reaction products, the consequences of this situation are quite distinct from those of a closed system where hydrolysing agents are steadily consumed with reaction progress. Nevertheless, since outputs for the closed system cases are considered in terms of rock/water ratios, we still gain some insight into the open system effect, as discussed below.

Specific reactant inputs into the programs include: (1) lake water sampled on 26 January 1990 (Table 1), including trace metal data from 17 November 1989 (Table 2); (2) andesite, with chemistry represented by the analysis of pumice bomb P38489 (Table 4; average trace element values for intermediate rocks from Roe 1983); and (3) vapour composition from White Island fumarole #3. We feel justified in using fumarolic data from White Island owing to the tectonic and petrogenetic similarities of the two volcanos (Cole 1979). Samples from the 354° C fumarole on White Island (Table 5) were collected and analysed according to methods described in Giggenbach and Goguel (1989). Trace metal data (Table 2) for this discharge are those of a condensate sample collected with a titanium and quartz glass sampling train.

Table 5. Fumarole Donald Mound #3, White Island, New Zealand

	2/12/88
H_2O	965330
CO_2	26100
S_t	6900
S_n	1.77
H_2S	2570
SO_2	4330
HCl	1320
HF	34
NH_3	0.7
H_2	69
Ar	0.3
N_2	246
CH_4	10

Sampling temperature = 354° C, units μmole/mole discharge. S_t stands for total sulfur, S_n is the average oxidation state of the sulfur species

Saturation state of the lake water

Figure 8 compares saturation indices and respective lake water temperatures for five samples collected between 1971–1973, and four samples collected between 1988–1991. Since reduced sulfur values are unavailable for the 1970s data (Giggenbach 1974), a constant value of 0.08 mg/kg was used for each of the 1970s samples, equal to the maximum observed values from the 1988–1990 period (Table 1). As SOLVEQ and CHILLER were both run using the H_2S-SO_4 redox buffer, this estimated value may introduce some bias into the calculated indices, particularly with respect to the sulfide minerals. However, it can be shown that it is the metal concentrations which dominate the calculated log (Q/K) values for the sulphide minerals at the low pH and relatively high oxidation potential in the lake. Therefore, if we assume that the 1970s aqueous reduced sulfur concentrations were within two orders of magnitude of the 1988–1990 values, the log Q/Ks for the two periods are considered comparable.

Outlet waters from both periods are close to saturation with respect to gypsum, amorphous silica and sulfur, consistent with observed mineral assemblage of the suspended load. Waters from both periods are saturated to moderately supersaturated with respect to orpiment and pyrite, but strongly supersaturated with

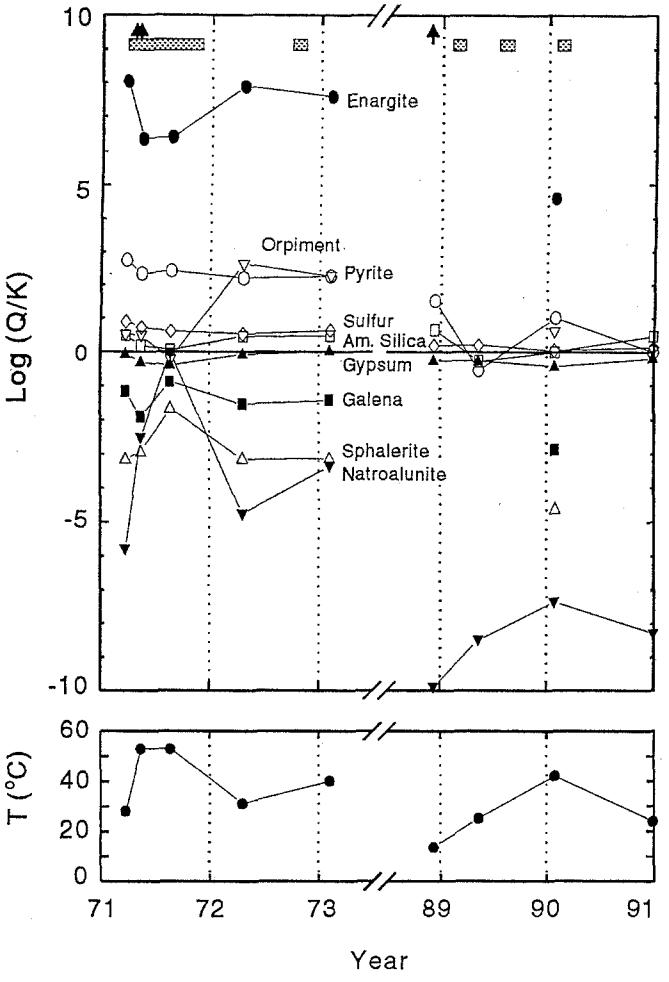

Fig. 8. Saturation indices of relevant alteration minerals for the two study periods. *Arrows* indicate major eruptive events, *stippled boxes* denote periods of hydrothermal activity

respect to enargite. The varying levels of supersaturation in these latter phases may represent, at least in part, quenching of a higher-temperature equilibrium condition, although the very high levels of enargite supersaturation may also reflect inaccurate or incomplete thermodynamic data for species involved in the solubility calculation. Galena and sphalerite are undersaturated at all temperatures.

Calculated values for the potassic end member of alunite, the only composition present in the SOLVEQ/CHILLER thermodynamic database, showed this phase to be strongly undersaturated at all temperatures. Assuming activity coefficients = 1 for the Na and K end member compositions, the log Q/K values were adjusted in the database for the natroalunite composition reported by Giggenbach (1974). The results show that natroalunite was closer to saturation in the 1970s than during the latter period. There is also a correlation between lake temperature and log Q/K, where the values are highest in both time periods when the lake is hot and actively convecting.

Base metal sulphide and sulph-arsenide saturation indices are generally lower in the later samples than in the 1970s. Several factors contribute to this change in-

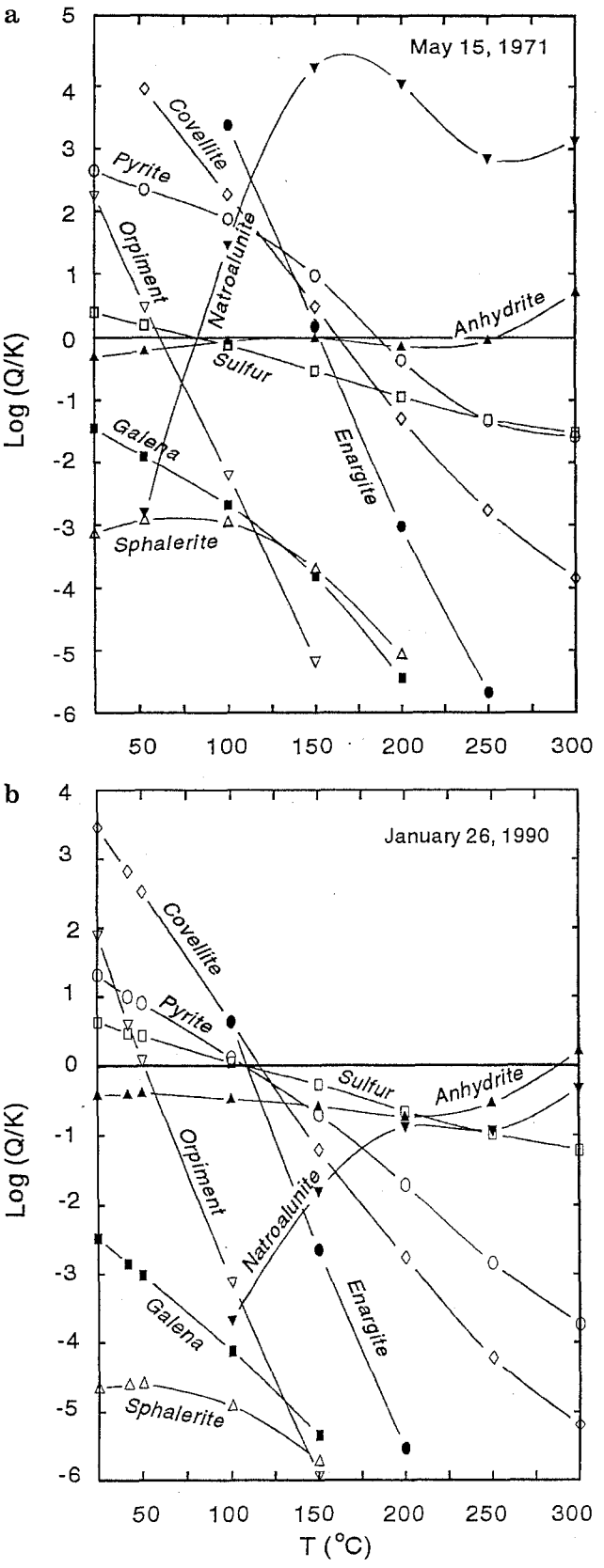

Fig. 9 a,b. Saturation state of lake water with conductive heating on 15 May 1971 (**a**) and 26 January 1990 (**b**). Saturation index (Log Q/K) values <0 reflect undersaturation with respect to specified mineral, values >0 indicative of supersaturation

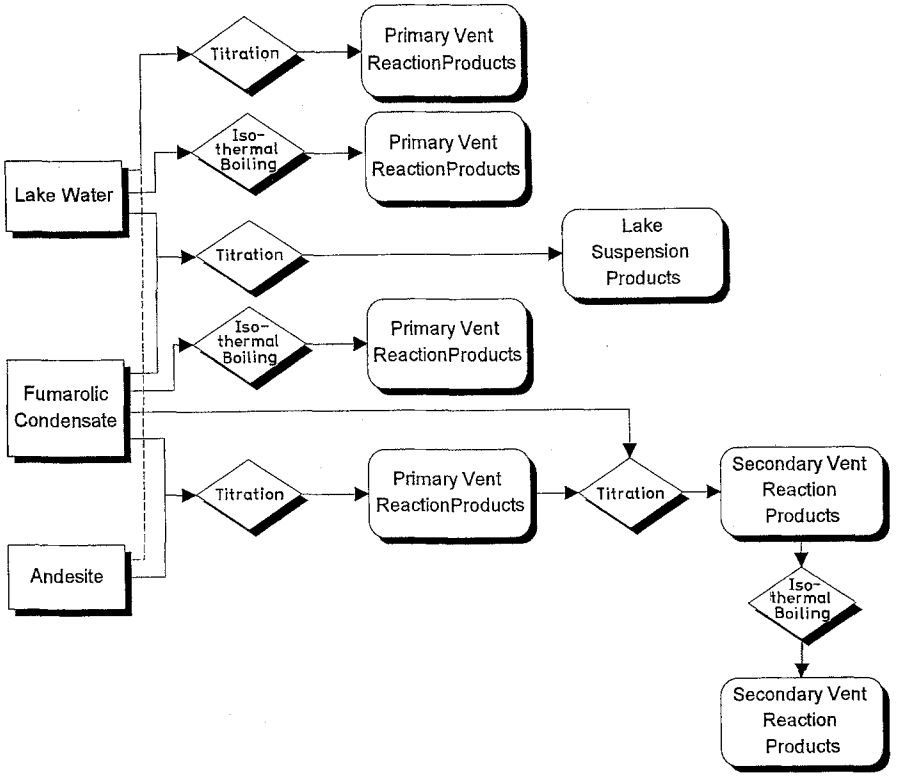

Fig. 10. Flow chart showing of reaction relationship modelled with CHILLER. *Rectangular* boxes enclose reactants and products, *diamond shapes* denote processes

cluding, as in the case of sphalerite and enargite, lower concentrations of the corresponding metal species in the later samples (Table 3 and Giggenbach 1974). However, pH variations through time are also of significance, which is especially true for natroalunite.

The temperature dependence on solubility of these phases is illustrated in Fig. 9 where the 15 May 1971 sample (Giggenbach 1974) is conductively heated using the SOLVEQ heating option. Convergence of saturation curves toward a common temperature at log (Q/K)=0 provides insight into previous equilibrium conditions of the fluid (Reed and Spycher 1984). Curves calculated for the May 1971 lake water, however, converge over a broad temperature range (ca. 80° C and 185° C), with the upper end of the range approximately coinciding with the lake-floor boiling-point temperature at the time. Saturation values (i.e. log Q/K=0) for pyrite, covellite and enargite occur at higher temperatures, and are interpreted as quenching of high temperature vent equilibria, whereas elemental sulfur, alunite, anhydrite (or gypsum) and amorphous silica appear to reequilibrate to varying extents in the lake. Galena and sphalerite diverge from the saturation conditon with increasing temperature, suggesting that they are not in the alteration assemblage in the shallow portions of the vent system.

The situation is different for the 26 January 1990 lake water, where covellite, enargite, and pyrite become undersaturated above 100–125° C, whereas natroalunite is undersaturated at all temperatures. This is interpreted to be the result of declining equilibrium temperatures along flow paths in the vent since 1971, and the lower pH of the fluid. The fact that there is little difference in sulfur equilibrium temperatures for the two time periods, on the other hand, suggests that the sulfur/lake water interface probably also existed at that time.

Reaction path models

Using the reactants outlined above, we use CHILLER to simulate the chemical consequences of four physical processes taking place in the vent (Fig. 10). These include: (1) dissolution reactions between fumarolic condensate and andesite and between lake water and andesite (environment B, Fig. 7); (2) mixing between high-temperature condensate and ambient lake water (environment 'C', Fig. 7); (3) mixing between unreacted condensate and that which has previously reacted with andesite (environments 'B' and 'C', Fig. 7); and (4) the effect of boiling on fluid–mineral relations for lake water and condensate.

Since fluid compositions change during precipitation or dissolution of mineral phases in reaction path calculations, it was necessary to use the potassic end member of the alunite solid solution series to represent this phase in the vent calculations. Although this increases the magnitude of changes in aqueous K concentrations for processes involving alunite (while leaving Na concentrations unaffected), the calculations are still highly relevant for identifying processes responsible for compositional variations in Crater Lake.

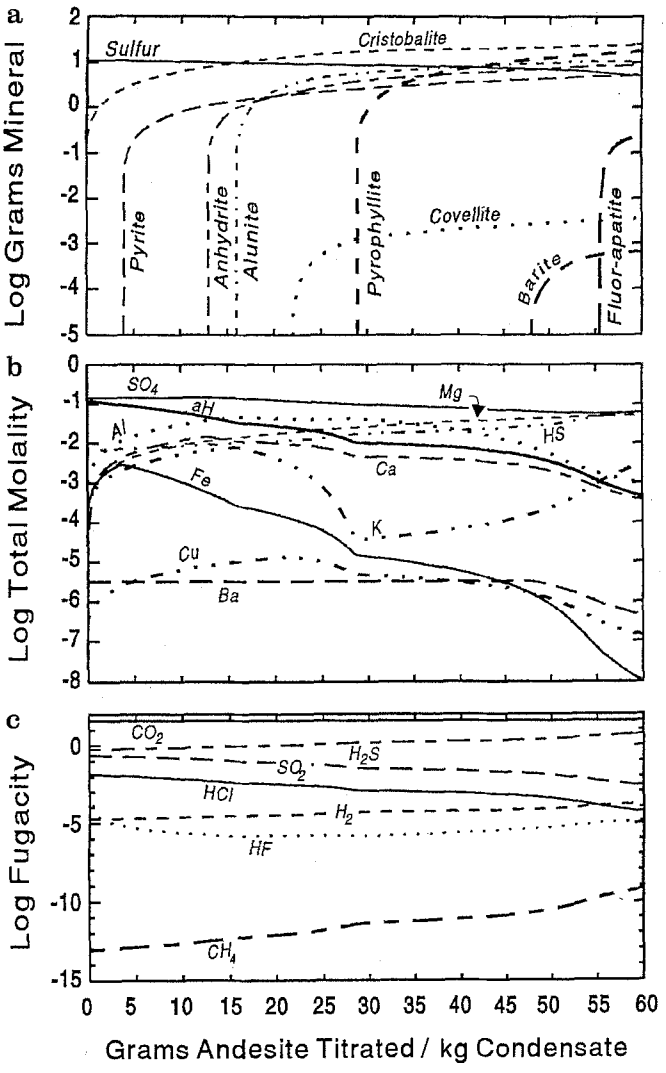

Fig. 11 a–c. Reaction path plots for fumarolic condensate–andesite reaction at 250° C

Condensate–Andesite reaction

The compositional pathways in Fig. 11a–c represent the changes in product minerals, total dissolved component species and gas fugacities respectively, during the titration of 60 g of Ruapehu andesite into 1 kg of high temperature condensate (the latter assumed to be equivalent to that discharging from White Island fumarole #3). This simulation was calculated at 250° C and 82 bars pressure, sufficient to retain all fumarolic gases in the condensed phase. In this and all subsequent runs, quartz, chalcedony, margarite and beidellite were excluded from the product matrix, consistent with their absence from eject samples.

The model calculation predicts that condensation of 1 kg of vapour is accompanied by the precipitation of more than 10 g of elemental sulfur; however, this phase subsequently redissolves as both aqueous sulfur species and hydrogen ions are consumed during the reaction. Cristobalite is the first phase to saturate, and thereafter controls activity of aqueous silica. The concentration of Fe in solution initially increases, but abruptly declines subsequent to the saturation of pyrite (at 4 g).

Anhydrite and alunite precipitate after 13 and 16 g of andesite are titrated respectively. The formation of alunite leads to the almost quantitative extraction of K from solution, controls the concentration of dissolved aluminium, and has a weakly stabilising influence on solution pH. However, the later precipitation of pyrophyllite competes with alunite for aqueous aluminium, resulting in a net increase in the concentration of K. Pyrophyllite further stabilises the solution pH, but this effect is soon superseded by the dissolution of alunite which occurs after ca. 50 g of andesite are titrated, leading to a relatively rapid increase in pH by about 1 unit by the time 60 g andesite are titrated.

SO_4 is steadily consumed during the dissolution of andesite, whereas total reduced S species increase, reflecting an overal shift in the redox potential of the system to more reducing conditions. This shift is also reflected in the fugacities of redox-sensitive gas species such as SO_2, which declines, and H_2S, H_2 and CH_4 which increase during the reaction.

Covellite saturates at 22 g, and steadily increases in quantity thereafter. Barite and fluorapatite are stabilised in the later stages, at 48 and 55 g respectively, where they become the sole controlling factors over Ba, PO_4 (not shown) and F concentrations.

Overall, 72.4 g of solids are produced from the dissolution of 60 g of andesite, with an overall increase in solution pH from ca. 0.9 to 3.3, while the Eh of the fluid decreases during the dissolution process. Hydroxyl-bearing alteration phases (e.g. alunite, pyrophyllite) influence, but do not buffer, the consumption of hydrogen ions throughout the dissolution process.

Continuing the calculation with a further 60 g of andesite results in the removal of elemental sulfur and alunite from the products, and the addition of clinochlore, galena and muscovite. The solution pH increases over this interval from 3.3 to 4.2. Since neither clinochlore or muscovite are observed in vent ejecta, it follows that the system has never been 'closed' enough with respect to fumarolic inputs to allow the reaction progress to achieve pH levels necessary to stabilise these phases.

While the major alteration products of the lake water–andesite reaction at 250° C are similar to those involving condensate, there are differences in the resulting ore phase assemblage caused by the higher redox potential of the lake water. Lake water rapidly saturates with respect to cristobalite, anhydrite, alunite and pyrophyllite, but does not begin to precipitate pyrite until 28 g of andesite are consumed. Hematite, which saturates after 47 g of andesite have been titrated, becomes the major iron-controlling phase. Total Fe concentration steadily increases until hematite saturates, which is in sharp contrast to the above example involving fumarolic condensate where iron is rapidly consumed by pyrite which precipitates early in the calculation. Gold and bornite both precipitate due to the low reduced S activity.

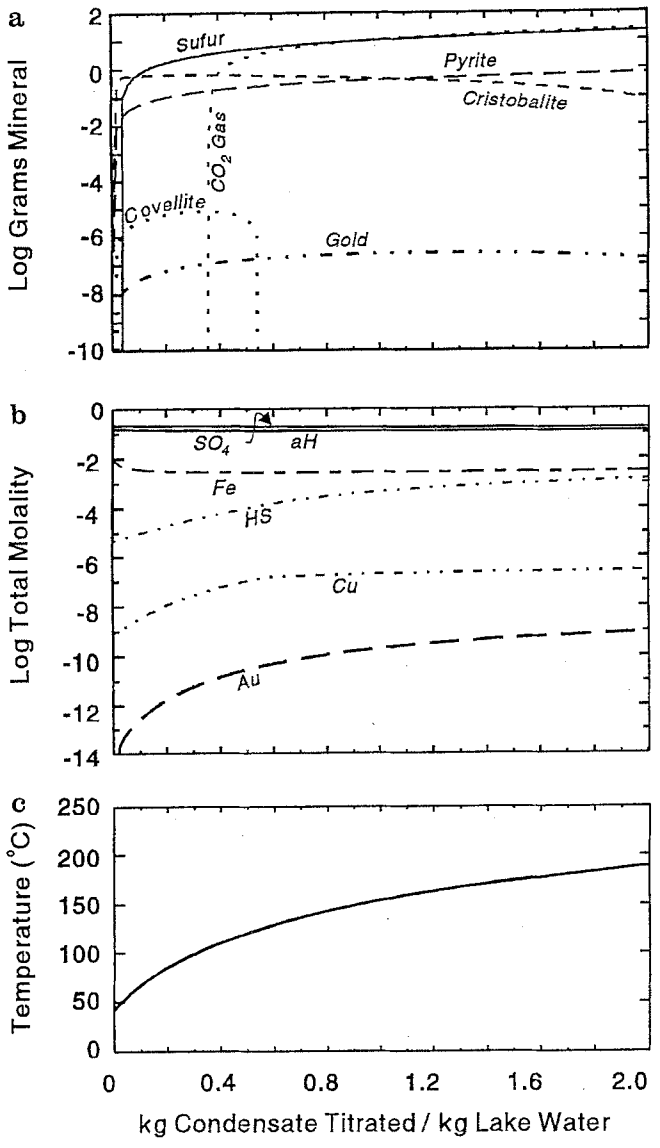

Fig. 12 a–c. Reaction path plot for fumarolic condensate–lake water mixing from 42° C

This modelling shows that dissolution of fresh andesitic material in the hydrothermal envelope results in the stepwise precipitation of a suite of alteration phases, most of which have been identified in vent ejecta (Table 3). Many of the compositional trends predicted by this modelling are broadly consistent with those observed in lake chemistry during and after the eruptions of 1971 (Figs. 4, 5); those that are slightly different, either in proportion (e.g. K, Fe and Al) or in magnitude (e.g. SO_4), indicate that other processes must also be involved.

Condensate–lake water mixing

Mixing of 250° C condensate with 42° C lake water is simulated in Fig. 12. The confining pressure for this calculation is 15 b, similar to that on the lake bottom in 1991. Pyrite, covellite and gold precipitate with the first aliquot of condensate titrated, followed by elemental sulfur in the next aliquot. Covellite is stable up to a condensate: lake water mass ratio of 0.55 (ca. 130° C), after which it redissolves completely. CO_2 saturates at mass ratio 0.36, before any other gas phase, consistent with the high CO_2 discharges sampled from the lake (Christenson, in press 1993). Elemental sulfur, gold and pyrite are present through mass ratio 2.0, although the latter two phases begin to redissolve in the later stages of the calculation.

Iron concentration abruptly decreases by a factor of about five at the beginning of the titration, consistent with the iron depletion observed in the lake water after the 1971 eruptions. SO_4 concentration and pH remain constant during the calculation, whereas total reduced sulfur concentration increases.

Comparison of these results to those where previously reacted condensate (60 g andesite/kg condensate) mixes with lake water shows only two significant differences: a more limited stability of precipitated gold (Au dissolves at mass ratio 1.14:1), and the appearance of alunite at mass ratio 1.96:1. In this case, gold dissolves due to the more reduced state of the reacted condensate (i.e. increased concentration of the reduced S ligand), whereas alunite precipitates due to the elevated K and Al concentrations of the reacted condensate.

Condensate–reacted condensate mixing

Introduction of fresh condensate into an environment containing reaction products from the dissolution of 60 g of andesite in 1 kg of condensate is simulated in Fig. 13. The earlier-formed fluor-apatite, barite and pyrophyllite are completely dissolved during the titration, whereas cristobalite and elemental sulfur are precipitated. Aluminium released from pyrophyllite, along with additional SO_4 from freshly introduced condensate, have an early stabilising effect on alunite. However, once pyrophyllite disappears, alunite also begins to dissolve, completely disappearing by mass ratio 2.75:1. Covellite, which steadily dissolves from the start of the run, disappears altogether by mass ratio 1.7:1.

The effects of the dissolution of the above minerals on solution chemistry are large (Fig. 13). There is a general increase in the calculated concentrations of all cations except K, which is first extracted from solution due to precipitation of alunite, but subsequently released after the disappearance of pyrophyllite. SO_4 and hydrogen ion activity increase during the run, whereas HS decreases, indicating that the fluid is again becoming more oxidised.

Observed changes in lake composition during the post-eruption recovery period of 1972–1973 and those of 1988–1990 (Fig. 4) are very similar to those presented here, and probably reflect dissolution of these previously formed alteration phases in the vent.

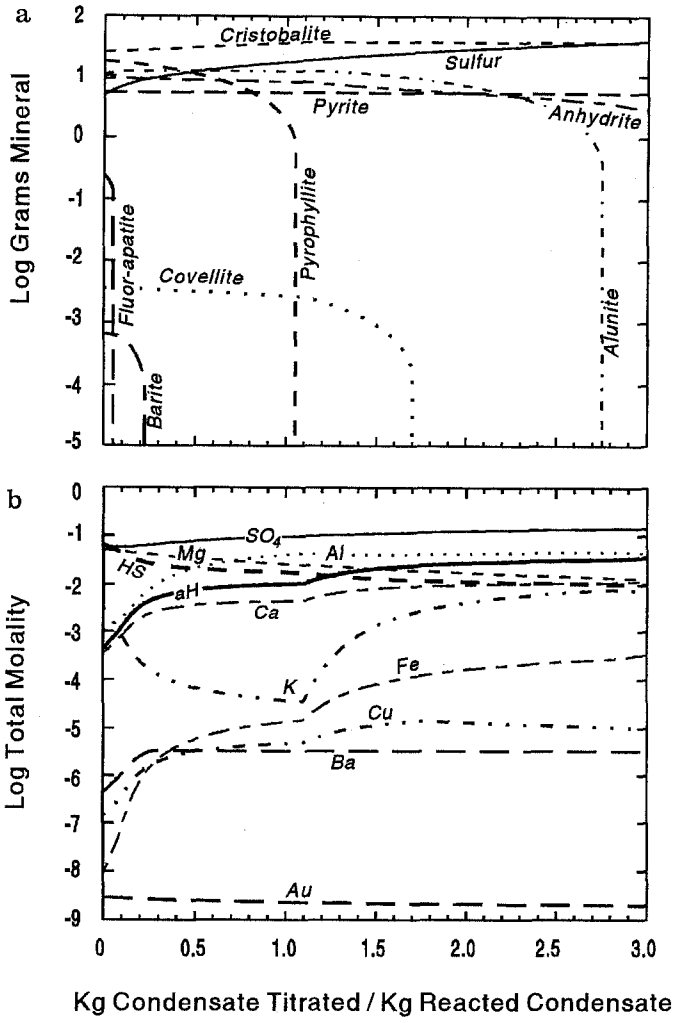

Fig. 13 a,b. Reaction path plot for the titration of fumarolic condensate into condensate previously reacted with 60 g andesite

Effects of boiling on vent fluid equilibrium relations

Boiling is expected to be a common occurrence in the vent environment, particularly during eruptive periods when vent temperatures increase and pressures fluctuate. Since the system is relatively open to both heat and mass in such circumstances, we consider isothermal boiling to be the most suitable heat balance situation to consider for chemical modelling purposes. In such a regime, there are no constraints against the fluid boiling to dryness, which poses some problems for modelling the process. Given the maximum ionic strength accommodated by the extended Debye–Huckle activity coefficient formulation used by CHILLER of about 4 molal (Spycher and Reed 1989), it is not possible to extend our modelling beyound this limit.

Isothermal boiling of lake water at 250° C reaches the limiting ionic strength of 4 molal at approximately 87% vapour loss, and requires a heat input of about 320 Kcal/kg of solution. Vapour loss causes immediate supersaturation of cristobalite, whereas anhydrite saturates at 29% vapour loss. Anhydrite precipitation continues until 83% of the solution is vaporised, after which it begins to redissolve. The pH steadily decreases from 1.08 to 0.84 by the time 83% of the mass is vaporised, but increases to 0.87 by the end of the run. This subtle pH behaviour at high salinity is linked to dissolution of anhydrite, where SO_4 from the dissolving anhydrite immediately associates with available protons to form the dominant sulfate species HSO_4.

Isothermal boiling of fumarolic condensate at 250° C is of little interest mineralogically in that the boiling process is roughly the reverse of condensation. It is interesting to note, however, that the 10.8 g of S initially precipitated in the condensate is completely volatilised (mainly to H_2S and SO_2) by the time 32% of the condensate mass is vaporised, indicating the relative ease with which S is mobilised in the vent environment.

The pH decreases only slightly over the boiling range considered here, from a starting value of 0.80–0.76 at 89% vapour loss. The pH stability is largely due to the loss of hydrolysis-promoting agents (e.g. HCl) from solution during boiling, countering the increase in hydrogen ions associated with vapour loss.

In contrast to pure condensate, boiling of previously reacted condensate (60 g of andesite/kg solution) induces some mineralogical and fluid compositional changes on the system (Fig. 14a). A number of the previously formed reaction products, including fluor-apatite, sulfur and pyrophyllite either partially or totally dissolve in the earliest stages of vapour loss (Fig. 14), and the consequent increase in SO_4 and Al activities leads to the precipitation of alunite. Covellite slowly dissolves during the run, whereas both gold and silver precipitate after 63% of the starting liquid mass is boiled to vapour.

The ionic strength of the solution increases from 0.14 to 1.7 molal with 83% vaporisation. The pH of the solution decreases from the initial value of 3.35 to 2.4 during the early dissolution of elemental sulfur, but then steadily increases to 2.7 at the completion of the run. The only conservative constituent in Fig. 14 is Mg, which steadily increases in concentration due to loss of solvent; all other species are affected in some way by fluid–mineral interaction or partitioning into the vapour phase. For example, K concentration abruptly decreases at the onset of boiling owing to the precipitation of alunite, whereas the concentration of Fe increases in concentration due to the dissolution of very small amounts of pyrite over the boiling interval. Cl, considered a conservative constituent in the lower temperature lake environment, is not conserved during boiling owing to the evolution of HCl gas. Since the volatility of HCl is an inverse function of pH (Truesdell et al. 1989), it appears necessary for acid neutralisation reactions to occur either prior to or simultaneously with boiling, if boiling is to play a significant role in the formation of highly concentrated Cl brines in the vent environment.

There is a net increase in redox potential in the liquid phase during boiling, as evident in the steady decrease in HS/SO_4. This is due largely to differential partitioning of the main redox controlling species (i.e.

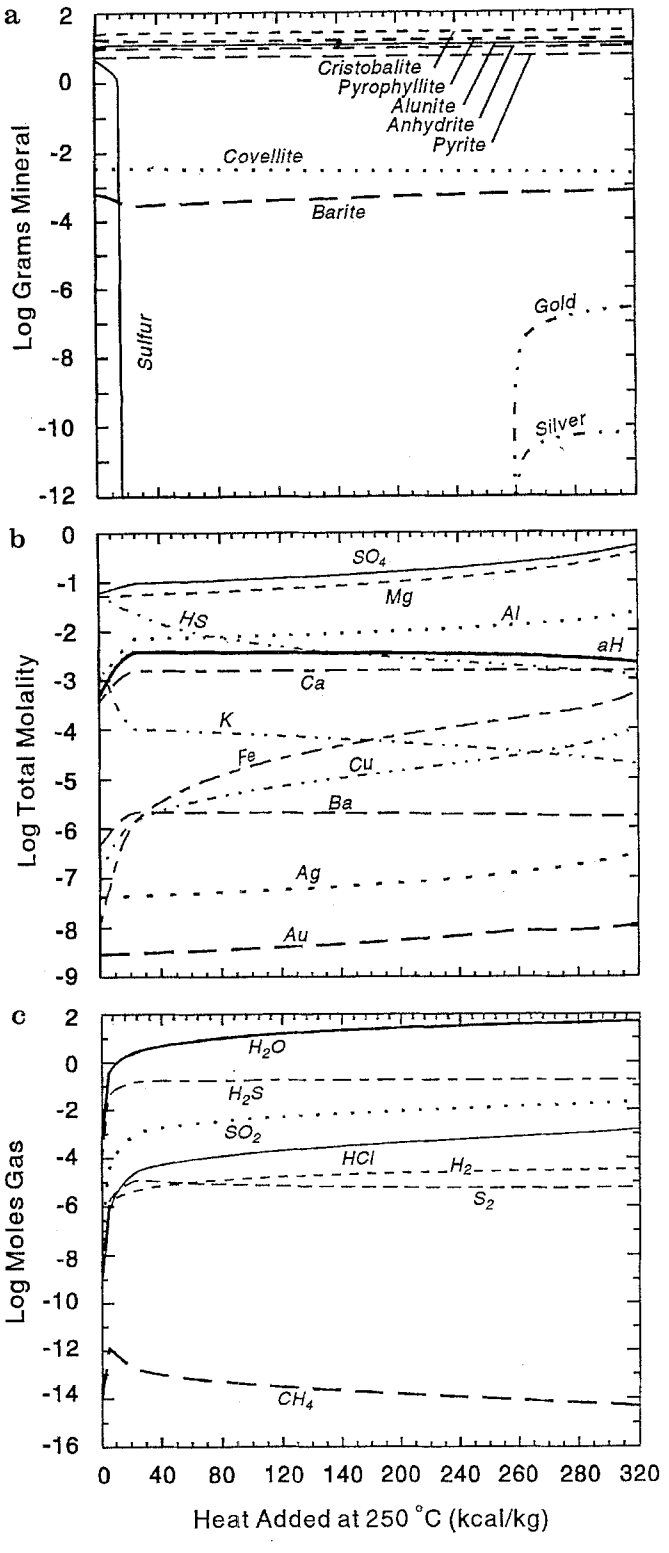

Fig. 14 a–c. Reaction path plot for closed system isothermal boiling (250° C) of condensate previously reacted with 60 g andesite

H_2S and SO_2) into the vapour phase; since SO_2 is about three times more soluble than H_2S at 250° C, it follows that the remaining liquid phase becomes more oxidising with vapour loss. The shifting redox potential during boiling is also evident in the equilibrium relations amongst evolved gases, most notably with the overall decline in CH_4 in the vapour/liquid system (Fig. 14c). Although total H_2 increases in the vapour/liquid system (Fig. 14c), the calculated (log) fugacity of H_2 in the liquid decreases from −3.7 to −4.6 during boiling, consistent with the shift to more oxidising conditions.

Relevance to ore-forming systems

The observed and modelled mineral assemblages in the vent/lake hydrothermal environment have many similarities to those found in high sulfidation-type gold deposits (Hedenquist 1987; White and Hedenquist 1990; Izawa 1991), and the range of modelled fluid compositions discussed above are nearly identical to those inferred for the Nansatsu District deposits in Japan (Hedenquist, in press 1993).

High sulfidation-type ore deposits are distinguished by their high total S contents, vuggy nature, advanced argillic mineral assemblages and disseminated ores of principally Cu and Au (White and Hedenquist 1990). While there have been no ore phases yet identified in ejecta from Ruapehu Crater Lake, the remaining characteristics bear close resemblance to the high sulfidation deposit criteria. Given the recent findings of pyrite, bismuthinite, stannite and enargite in sulfur from a similar crater lake on Kawah Ijen volcano, Indonesia (Delmelle and Bernard 1993), and the predicted assemblages discussed earlier, we suggest that the hitherto dearth of ore minerals from Ruapehu is an artefact of sampling.

Ore metals may be introduced into the volcanic hydrothermal system by either dissolution of primary andesitic material or by upwardly streaming, high-temperature gases from the underlying magma. Whereas it was shown above that andesite dissolution and associated vent processes can lead to the precipitation of ore minerals, the quantities of ore minerals generated in a single eruption cycle are small. Nevertheless, given sufficient time and eruptive activity a vent-hosted ore deposit could easily be formed in this way.

Andesite dissolution, condensate-lake water mixing and boiling of reacted condensate all lead to the precipitation of Cu ore minerals, but only condensate–lake water mixing and boiling of reacted condensate precipitate gold and/or silver in the above calculations. Although enargite, a very common phase in high sulfidation deposits, never appears as stable phase in the computed ore assemblages, it is always very close to saturation. The fact that covellite saturates first and subsequently controls Cu solubility may be due to the redox state of the system, faulty thermodynamic data for the Cu mineral phases, or perhaps the usage of non-representative As values in the calculations. Increasing the As concentrations in the White Island condensate by a factor of 10, for example, resulted in uniform enargite control of Cu solubility in the calculations.

High-temperature gas transport is a more direct means of introducing ore metals into the hydrothermal environment (Symonds et al. 1987; Gemmell 1987; Kyle et al. 1990). Whereas the above calculations used

the 345° C fumarolic discharge from White Island as a proxy for the magmatic gas phase entering the saturated two-phase zone in the vent of Ruapehu, these gases would have already lost significant quantities of ore constituents through sublimation processes in transit to the vent (e.g. Symonds et al. 1987). Whereas high-temperature sublimation effectively precludes the potential ore metals from reaching the saturated hydrothermal (i.e. ore-forming) environment, expansion and collapse of the single phase vapour zone (cf. Fig. 7) with cyclic eruptive activity may eventually bring the sublimates into contact with circulating vent liquids, leading to redistribution of ore metals into a deposit of the high sulfidation-type.

Conclusions

Arguments presented here concerning the physical and chemical vent processes are consistent with the views of Hurst et al. (1991) regarding the nature of the heat source in Ruapehu, i.e. that a heat pipe convectively transfers heat between the magma body and the lake. Indeed, changes in lake composition during comparatively quiescent periods suggest that lake water circulates through the upper portion of the vent and dissipates heat from the condensation zone of the heat pipe. The term 'leaking heat pipe' has been applied here to account for the destabilising effects of non-condensable gas pressures on the operation of the heat pipe, although the effects of these gases on the cyclic nature of the heat flow to the lake deserves further study.

There is a clear correlation between compositional changes in Crater Lake chemistry and eruptive events (Giggenbach 1974; and Giggenbach and Glover 1975). We have presented further data and arguments which show the variations in lake chemistry are the result of ongoing reaction path processes in the vent-lake system.

Condensation of upwardly steaming magmatic volatiles leads to the precipitation of elemental sulfur, and the formation of an acidic solution comprised largely of sulphuric and hydrochloric acids. Thermodynamic modelling shows that dissolution of fresh andesitic material in the vent by condensate and/or recirculating lake water leads to the formation of a distinctive assemblage of alteration minerals, many of which have been identified in vent ejecta. In a closed chemical system at 250° C, this assemblage consists of cristobalite, pyrite, anhydrite, alunite and pyrophyllite. As the fluid becomes increasingly acid neutralised and reduced through reaction with the andesite, the rocks become increasingly oxidised.

The equilibrium alteration assemblage will reflect the degree to which the system remains open to hydrolysis-promoting agents (i.e. acid condensate); the phase least sensitive to acid attack in this regard is cristobalite, whereas that most sensitive to hydrolysis in the above assemblage in pyrophyllite. If andesite in the reaction environment is largely converted to the above assemblage, and if reaction with fresh condensate continues, the previously formed alteration products will redissolve in approximately the reverse order to that listed above. This appears to have occurred, in part, during 1972 and again during the two-year period following the vent-clearing eruption of 1988, with the dissolution of natroalunite.

Equilibrium calculations presented here also indicate that processes in the hydrothermal environment of the vent are conducive to the formation of high sulfidation-type ore assemblages. Apart from the aforementioned advanced argillic assemblage minerals, the ore phases covellite, gold and silver precipitate in several of the reaction scenarios described above, and enargite is very close to saturation in most scenarios. Although details of metal transport into the reaction environment should receive further attention, we suggest that the active crater lake environment is a good analogue for the high-sulfidation-type ore depositing environment.

Acknowledgements. We wish to thank Werner Giggenbach for his insights into the workings of Crater Lake and manuscript review, Mark Reed for insights into the computer modelling, and RB Glover, JW Hedenquist, M Kusakabe for their reviews of the manuscript. We acknowledge ME Crump and AL Trewick for their assistance with chemical analyses, and PM Otway, IA Nairn and BJ Scott for their help with sampling during this project. Finally, we acknowledge the work of numerous DSIR staff who over the years have contributed great effort to the maintenace of the Ruapehu monitoring program.

References

Blount CW, Dickson FW (1973) The solubility of anhydrite ($CaSO_4$) in NaCl-H_2O from 100 to 450C and 1 to 1000 bars. Am Mineral 62:942–957

Burnham CW (1979) Magma and hydrothermal fluids. In: Barnes HL (ed) Geochemistry of hydrothermal ore deposits. John Wiley & Sons, New York, pp 71–137

Christenson BW (1993) Convection and stratification in Ruapehu Crater Lake, New Zealand: Implications for Lake Nyos-type gas release eruptions. In press, Chem Geol

Christenson BW, Crump ME, Glover RB (1992) Ruapehu Crater Lake bathymetry, temperature profile and water column chemistry: February 1991. Proc Intnl Symp on Hazardous Crater Lakes, Misasa and Tateyama, Japan, 1992, pp 25–29

Cole JW (1979) Structure, petrology, and genesis of Cenozoic volcanism, Taupo Volcanic Zone, New Zealand – a review. NZ J Geol Geophys 22:631–657

Cole JW, Nairn IA (1975) Catalogue of the active volcanos of the world including solfatara fields – Part 22: New Zealand. IAVCEI, Naples, pp 1–156

Demelle P, Bernard A (1993) A thermodynamic modelling study of the Kawah Ijen acid crater lake, Java, Indonesia. Terra Abs, EUG VII, Strasbourg, 1993

Eastman GY (1968) The heat Pipe. Sci Am 218(5):38–57

Gemmell JB (1987) Geochemistry of metallic trace elements in fumarolic condensates from Nicaraguan and Costa Rican volcanoes. J Volcanol Geotherm Res 33:161–181

Giggenbach WF (1974) The chemistry of Crater Lake, Mt Ruapehu (New Zealand) during and after the 1971 active period. NZ J Sci 17:33–45

Giggenbach WF, Glover RB (1975) The use of chemical indicators in the surveillance of volcanic activity affecting the crater lake on Mt. Ruapehu, New Zealand. Bull Volcanol 39:70–81

Giggenbach WF, Goguel RL (1989) Collection and analysis of geothermal and volcanic water and gas discharges. DSIR Chem Div Report CD2401, pp 1–81

Giggenbach WF, Sheppard DS (1989) Variations in temperature and chemistry of White Island fumarole discharges 1972–1985. NZ Geol Surv Bull 103:119–126

Gregg DR (1960) Volcanos of Tongariro National Park. DSIR Geol Surv Handbook Info Series 28:1–82

Healy J, Lloyd EF, Rishworth DEH, Wood CP, Glover RB, Dibble RR (1978) THe eruption of Ruapehu, New Zealand, on 22 June 1969. DSIR Bull 224:1–80

Hedenquist JW (1987) Mineralisation associated with volcanic-related hydrothermal systems in the circum-Pacific Basin. In: MK Horn (ed), Transactions of the Fourth Circum-Pacific Energy and Mineral Resources Conference, Singapore. Am Assoc Pet Geol, pp 513–524

Hedenquist JW, Matsuhisa Y, Izawa E, White NC, Giggenbach WF, Aoki M (1993) Geology and geochemistry of high sulfidation Au-Cu mineralisation in the Nansatsu district, Japan. In press, Econ Geol

Hurst AW, Bibby HM, Scott BJ, McGuiness MJ (1991) The heat source of Ruapehu Crater Lake; deductions from the energy and mass balances. J Volcanol Geotherm Res 6:1–21

Hurst AW, Dibble RR (1981) Bathymetry, heat output and convection in Ruapehu Crater Lake, New Zealand. J Volcanol Geotherm Res 9:215–236

Ingebritsen SE, Sorey ML (1988) Vapour-dominated zones within hydrothermal systems: evolution and natural state. J Geophys Res 93:13635–13655

Irwin J (1972) New Zealand lakes bathymetry survey 1965–1970. NZ Oceanogr Inst Rec 1(6):107–126

Izawa E (1991) Hydrothermal alteration associated with Nansatsu-type gold mineralisation in the Kasuga area, Kagoshima Prefecture, Japan. In: Matsuhisa Y, Aoki M, Hedenquist UW (eds) High-temperature acids fluid and associated alteration and mineralisation. Geol Surv Japan Rep No. 277, 11 pp

Kiyosu Y, Kurahashi M (1983) Origin of sulfur species in acid SO_4-Cl thermal waters, north eastern Japan. Geochim Cosmochim Acta 47:1237–1245

Kyle PR, Meeker K, Finnegan D (1990) Emission rates of sulfur dioxide, trace gases and metals from Mount Erebus, Antarctica. Geophys Res Letters 17:2125–2128

McGuinness MJ, Pruess K (1987) Unstable heatpipes. Prosc 9th NZ Geoth Workshop, Auckland University, Auckland, pp 147–151

McKibben R, Preuss K (1988) On non-condensable gas concentrations and relative permeabilities in geothermal reservoirs with gas-liquid co- or counterflows. Procs 10th NZ Geothermal Workshop, Auckland University, pp 1–8

Mizutani Y, Sugiura T (1966) The chemical equilibrium of the $2H_2S+SO_2=3S+2H_2O$ reaction in solfataras of the Nasudake Volcano, Hokkaido, Japan Bull Chem Soc Japan 39:2411–2414

Nairn IA (1982) 1982 bathymetric soundings. DSIR Immediate Report

Nairn IA, Wood CP, Hewson CAY (1979) Phreatic eruptions of Ruapehu: April 1975. NZ Geol Geophys 22:155–173

Pitzer KS, Pabalan RT (1986) Thermodynamics of NaCl in steam. Geochim Cosmochim Acta 50:1445–1454

Reed MH (1982) Calculation of multicomponent chemical equilibria and reaction processes in systems involving minerals, gases and an aqueous phase. Geochim Cosmochim Acta 46:513–528

Reed MH, Spycher NF (1984) Calculation pH and mineral equilibria in hydrothermal waters with application to geothermometry and studies of boiling and dilution. Geochim Cosmochim Acta 48:1479–1492

Roe HJ (1983) Lehrbuch für Mineralogie. Für Grundstoffindustrie, Leipzig, pp 1–534

Spycher NF, Reed MH (1989) Evolution of a Broadlands-type epithermal ore fluid along alternative P-T paths: Implications for the transport and deposition of base, precious and volatile metals. Econ Geol 84:328–359

Symonds RB, Rose WI, Reed MH, Lichte FE, Finnegan DL (1987) Volatilisation, transport and sublimitation of metallic and non-metallic elements in high temperature gases at Merapi Volcano, Indonesia. Geochim Cosmochim Acta 51:2083–2101

Takano B, Watanuki K (1989) Monitoring of volcanic eruptions at Yugama crater lake by aqueous sulfur oxyanions. J Volcanol Geotherm Res 40:71–87

Truesdell AH, Haislip JR, Armannsson H, D'Amore F (1989) Origin and transport of Cl^- in superheated geothermal steam. Geothermics 18:295–304

Webster JG (1989) An analytical scheme for the determination of sulphide, polysulphide, thiosulfate, sulphite and polythionate concentrations in geothermal waters. DSIR Chem Div Rep CD2406, pp 1–18

White NC, Hedenquist JW (1990) Epithermal environments and styles of mineralisation: variations and their causes, and guidelines for exploration. J Geochem Explor 36:445–474

Wood CP (1975) Ruapehu: Andesitic glass foam. 1973 DSIR NZ Volcanological Rec 3:38–39

Editorial responsibility: W. F. Giggenbach